

# Study of red-emitting LaAsO<sub>4</sub>:Eu<sup>3+</sup> phosphor for color rendering index improvement of WLEDs with dual-layer remote phosphor geometry

My Hanh Nguyen Thi<sup>1</sup>, Nguyen Thi Phuong Loan<sup>2</sup>, Nguyen Doan Quoc Anh<sup>3</sup>

<sup>1</sup>Faculty of Mechanical Engineering, Industrial University of Ho Chi Minh City, Viet Nam

<sup>2</sup>Faculty of Fundamental 2, Posts and Telecommunications Institute of Technology, Vietnam

<sup>3</sup>Power System Optimization Research Group, Faculty of Electrical and Electronics Engineering, Ton Duc Thang University, Vietnam

## Article Info

### Article history:

Received Jul 19, 2019

Revised Jun 30, 2020

Accepted Jul 9, 2020

### Keywords:

Color rendering index

Dual-layer remote phosphor geometry

LaAsO<sub>4</sub>:Eu<sup>3+</sup>

Mie-scattering theory

WLEDs

## ABSTRACT

The remote phosphor structure is often disadvantageous in color quality but in terms of optics it is more convenient when compared to other phosphor structures such as conformal or in-cup ones. From this disadvantage, there are many studies to improve its chromatic output. In this research paper, we propose a dual-layer remote phosphor geometry for the improvement of white light-emitting diodes (WLEDs) in two parameters: color rendering index (CRI) and color quality scale (CQS). The 7700 K WLEDs are used in this study. The idea of the study is to place a red phosphor layer LaAsO<sub>4</sub>:Eu<sup>3+</sup> on the yellow phosphor YAG: Ce<sup>3+</sup>, and then find the concentration of LaAsO<sub>4</sub>:Eu<sup>3+</sup> in an appropriate way to achieve the highest color quality. The results showed that LaAsO<sub>4</sub>:Eu<sup>3+</sup> bring great benefits for enhancing CRI and CQS. In particular, the greater the concentration of LaAsO<sub>4</sub>:Eu<sup>3+</sup>, the greater the CRI and CQS because the portion of red lights in WLEDs increases. However, the decrease in lumen output occurs when the concentration of LaAsO<sub>4</sub>:Eu<sup>3+</sup> increases excessively. This is proved thanks to Mie-scattering theory and Beer-Lambert law. The results of important articles in WLEDs fabrication have greatly contributed to a higher white light quality

This is an open access article under the [CC BY-SA](https://creativecommons.org/licenses/by-sa/4.0/) license.



## Corresponding Author:

Nguyen Doan Quoc Anh,  
Power System Optimization Research Group,  
Faculty of Electrical and Electronics Engineering,  
Ton Duc Thang University,  
Ho Chi Minh City, Vietnam.  
Email: nguyendoanquocanh@tdtu.edu.vn

## 1. INTRODUCTION

As seen, phosphor-converted white light-emitting diodes (WLEDs) is a fourth-generation source of illumination and a potential for replacing the conventional one that has a variety of prospects in lighting solution [1]. The application of white light-emitting diodes has spread to many different fields of our life, for example, lighting equipment for landscape and street, or backlighting. Yet, there are existing obstacles related to the light extraction efficiency and the homogeneity of angular-dependent correlated color temperature (CCT) for white light emitting diodes (LEDs), which is the primary cause that limits their development [2]. As the lighting market continues to develop, the standards for WLEDs in use become higher and higher, and so, further breakthroughs in luminous efficiency and color quality are really essential [3]. An approach that is very

common in today's lighting technology is the one based on the idea of combining yellow lights from yellow emitting phosphor with blue lights from blue LED chips. Though this is a familiar concept, the importance in the way a LED package is constructed and the phosphor layers are arranged is undeniable. It is because these factors have significant impacts on the performance of LED lights, including lumen efficacy and color rendering index (CRI) [4-8]. Capturing this concept, several common phosphor coating methods have been introduced and investigated to manufacture WLED packages, for examples, the dispensing and conformal coating approaches [9, 10]. Nevertheless, these structures do not provide high color quality because the direct contact of the phosphor layers and the LED chips in the LED packages causes the thermal increase at their junction and then leading to the degraded internal light conversion. Thus, the reduction in heating outcome can help to enhance the efficiency of phosphor layers and prevent them against being irreversibly damaged. Many previous studies have established that the remote phosphor structure designed with a phosphor layers placed distantly from the LED chips' surface, also known as the heat source, probably reduces the effect of heating. An appropriate gap between the phosphor and the LED chip will help LED lights limit the internal backscattering and circulation of light rays. Hence, this approach can be one of most optimal solutions for internal thermal control of WLEDs. Moreover, the lumen efficacy and color quality of WLEDs can be promoted when this method is applied successfully [11-16]. Nonetheless, it seems that the former structure utilizing the remote phosphor technology can only serve the specifications of conventional lighting devices.

In other words, they may not completely fulfill other requirements of other modern lighting applications. Therefore, the next WLED generation needs to be investigated and fabricated. For further development, several new models of remote phosphor structure have been suggested to reduce the phosphor-emitting lights scattering back to the LED chip's surface and increase the efficacy of luminous flux. In a previous study, it is presented that by using an encapsulation of inverted cone lens combined with a ring-shaped remote phosphor film, the light from the LED chips to the device's surface can be redirected, and this leads to the decrease in the light loss caused by the internal reflection [17]. Meanwhile, when using a patterned structure for remote phosphor configuration together with a non-phosphor-coated region in the perimeter area, a higher homogeneity of angular CCT and better color consistency could be achieved [18]. In addition, that the patterned sapphire substrate used in the remote phosphor is an advantage factor to get the color uniformity in the far field better than that in the conventional field [19-21]. Though, these aforementioned studies concentrate on the improvement of chromatic homogeneity and the lumen output of WLEDs with remote phosphor structure, they just demonstrated the results researched only on WLED packages with single LED chip and low color temperatures. Meanwhile, it is difficult and complicated for high-color-temperature WLEDs to accomplished the enhancement in their optical properties.

Acknowledging the obstacles, our paper proposes a dual-layer remote phosphor structure to improve color quality for 7700 K WLEDs. The new idea of the paper is to use the red  $\text{LaAsO}_4:\text{Eu}^{3+}$  phosphor layer for obtaining the increase in red light components of WLEDs, resulting in the higher color rendering index (CRI) and color quality scale (CQS). The results present that CRI and CQS were significantly improved when added phosphor  $\text{LaAsO}_4:\text{Eu}^{3+}$ . However, it is necessary to select the concentration  $\text{LaAsO}_4:\text{Eu}^{3+}$  which is suitable to avoid the deep decrease of luminous flux when redundant phosphor concentration is excessive. There are three differences when adding red phosphor to yellow  $\text{YAG}:\text{Ce}^{3+}$  phosphor layer. The first is that the red light component increases, which increases the spectrum of red light area emitted by the white light range. This is the key to increasing color performance of WLEDs. The second is the scattering ability and the transmission of light rays in WLEDs are inversely proportional to the concentration of  $\text{LaAsO}_4:\text{Eu}^{3+}$ . Therefore, the appropriate concentration of  $\text{LaAsO}_4:\text{Eu}^{3+}$  becomes important for maintaining the luminous flux of WLEDs.

## 2. PREPARATION AND SIMULATION

It is vital to apply the LightTools program and Mie-theory into this work. It helps WLEDs with dual-layer phosphor structure be easily simulated through analyzing the scattering of phosphor particles and supports the process of investigating the influence of  $\text{LaAsO}_4:\text{Eu}^{3+}$  phosphor on the performance of the WLEDs at the high correlated temperature of 7700 K. In order to prepare for the process of the in-cup phosphor configuration of WLEDs, we blend the  $\text{LaAsO}_4:\text{Eu}^{3+}$  and  $\text{YAG}:\text{Ce}^{3+}$  phosphor compounding as expressed in Figure 1. Consequently, the phosphor layer of WLEDs contains  $\text{LaAsO}_4:\text{Eu}^{3+}$  phosphor,  $\text{YAG}:\text{Ce}^{3+}$  phosphor, and silicone glue. The constituents of simulated WLEDs expressed in the model are blue chips, a reflector cup, one layer of phosphor, and one layer of silicone. A reflector, with a 2.07 mm depth, a bottom length of 8 mm and a length of 9.85 mm at its top surface, is bonded with the blue chip whose radiant power is 1.16 W, and the highest wavelength is at 453 nm. Meanwhile, 18.85 and 18.3 are refractive indices of  $\text{LaAsO}_4:\text{Eu}^{3+}$  and  $\text{YAG}:\text{Ce}^{3+}$ , respectively. To maintain the average CCTs, the  $\text{YAG}:\text{Ce}^{3+}$  phosphor concentration need to change appropriately to the concentration of  $\text{LaAsO}_4:\text{Eu}^{3+}$ .

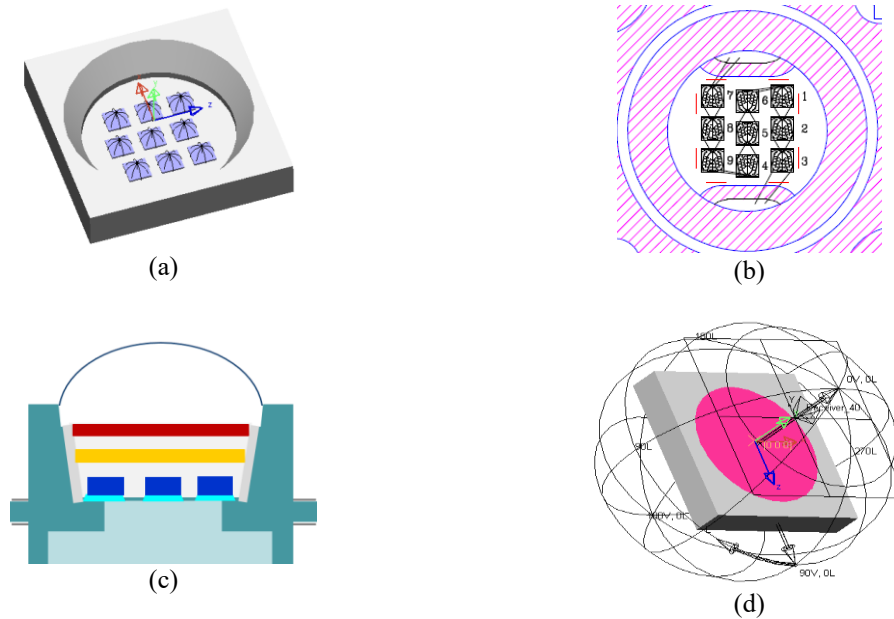


Figure 1. Illustrated WLED structure; (a) 3D modelling, (b) bonding diagram, (c) graphic pc-WLEDs model, (d) simulation of a WLED with LightTools software

### 3. RESULTS AND DISCUSSION

Shown in Figure 2 is the opposite changing trends between red phosphor concentration  $\text{LaAsO}_4:\text{Eu}^{3+}$  and yellow phosphor  $\text{YAG}:\text{Ce}^{3+}$ . This change has two meanings: the first is to maintain the average CCTs; the second is that the scattering and absorption of phosphor layers are affected by this change. This certainly affects the color quality and output of WLEDs. Thus, the concentration selection of  $\text{LaAsO}_4:\text{Eu}^{3+}$  determines the color quality of WLEDs. When concentration  $\text{LaAsO}_4:\text{Eu}^{3+}$  increases from 2% to 26% wt., the concentration of  $\text{YAG}:\text{Ce}^{3+}$  tends to decline for maintaining average CCTs, and this also happens to the WLEDs with color temperature of 7700 K.

The most obvious effect of the red phosphor concentration  $\text{LaAsO}_4:\text{Eu}^{3+}$  on the spectral transmission of WLEDs is shown in Figure 3. Depending on the manufacturer's requirements, the choice is made. WLEDs with high color quality requirements can reduce a small amount of luminous flux. White light is the synthesis of the spectral region as shown in Figure 3. This image shows luminous flux of 7700 K. Red region from 648 nm to 738 nm increases with  $\text{LaAsO}_4:\text{Eu}^{3+}$  concentration. However, this is not significant without the spectral increase of the two remaining regions of 420-480 nm and 500-640 nm. The spectral increase of the two 420-480 nm regions increases the luminous flux of blue light (blue-light scattering). The higher the color temperature, the higher the spectral emission. This is an important result when applying  $\text{LaAsO}_4:\text{Eu}^{3+}$  to control the color quality of WLEDs with high temperature. This study confirms the ability of  $\text{LaAsO}_4:\text{Eu}^{3+}$  in yielding better color performance for WLEDs with both low (5600 K) and high (7700 K) color temperatures.

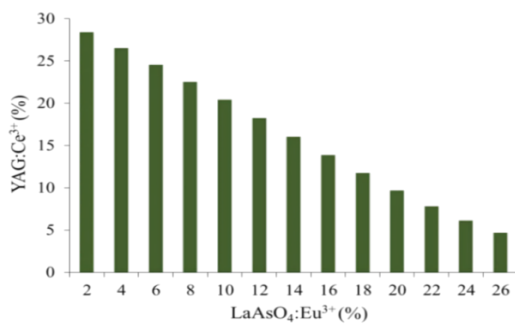


Figure 2. The change of phosphor concentration for keeping the average CCT

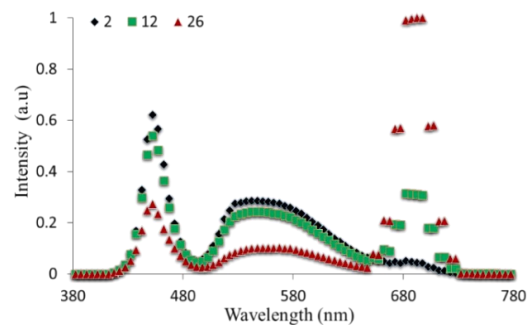


Figure 3. The emission spectra of 7700 K WLEDs as a function of  $\text{LaAsO}_4:\text{Eu}^{3+}$  concentration

Figure 4 describes that the color rendering indices increase with  $\text{LaAsO}_4:\text{Eu}^{3+}$  phosphor content in the structure. This can be explained by the absorption of the red phosphor layer: the blue lights from LED chips are turned into red lights after being absorbed by the red phosphor  $\text{LaAsO}_4:\text{Eu}^{3+}$ . Besides that,  $\text{LaAsO}_4:\text{Eu}^{3+}$  still absorbs the yellow lights. However, when drawing a comparison between these two absorptions, blue lights from LED chips are absorbed more strongly owing to the absorption properties of the red phosphor, and thus there is an obvious increase in red light components in WLEDs when adding  $\text{LaAsO}_4:\text{Eu}^{3+}$ . It leads to increased color rendering index (CRI). In the parameters of selecting modern WLED lamps, color rendering index plays an important role, leading to the fact that the higher the CRI values WLEDs have, the more expensive the WLED devices become. Moreover, using  $\text{LaAsO}_4:\text{Eu}^{3+}$  has another benefit which is low cost. Therefore,  $\text{LaAsO}_4:\text{Eu}^{3+}$  can be widely used, but that's not to say high CRI certainly leads to good color quality.

The reason is that this reimbursement index is only one factor to evaluate the color quality of WLEDs, or in other words, it is not completely accurate to classify the grade of color performance for WLED with only CRI. Therefore, the current studies have come up with a new potential parameter that is CQS that is comprised of three factors: the first is the CRI factor, the second is the preference from viewers, and the last one is the color coordinates. Thanks to the combination of these three important elements, CQS is almost a true overall color quality index. Figure 5 shows CQS enhancement in the presence of the remote phosphor  $\text{LaAsO}_4:\text{Eu}^{3+}$  layers. And when increasing concentration  $\text{LaAsO}_4:\text{Eu}^{3+}$ , CQS also increased significantly. Clearly, using  $\text{LaAsO}_4:\text{Eu}^{3+}$  can increase the quality of white-light color of a WLED package with a dual-layer phosphor structure. This is the crucial outcome of the research when the improvement of color quality is one of the focusing objectives. However, it is impossible not to consider the disadvantages of  $\text{LaAsO}_4:\text{Eu}^{3+}$  to emitted luminous flux. In the next part are the demonstrations of the mathematical model which is used to calculate the transmitted blue lights and converted yellow lights of the dual-layer remote configuration, and this also can help to achieve a huge enhancement of WLED efficiency.

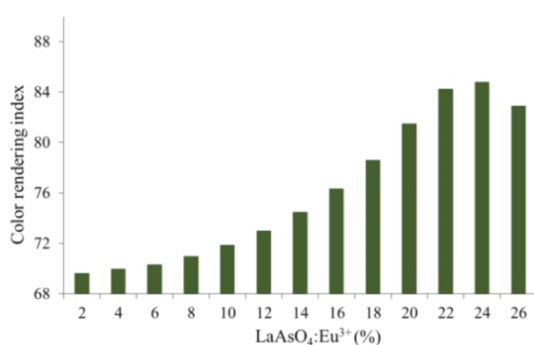


Figure 4. Color rendering indices of WLEDs in accordance with  $\text{LaAsO}_4:\text{Eu}^{3+}$  concentration

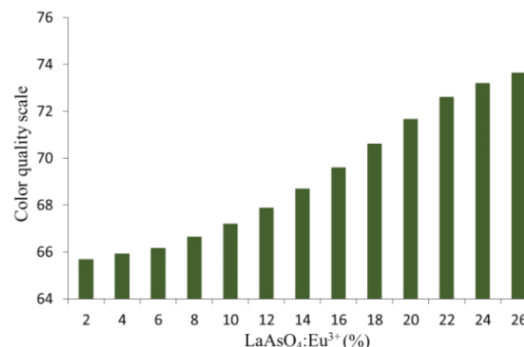


Figure 5. The color quality scale of WLEDs in accordance with  $\text{LaAsO}_4:\text{Eu}^{3+}$  concentration

In terms of the transmitted blue lights and converted yellow lights of a single-layer remote design, the computation can be presented as the following, given that its phosphor film has a thickness of  $2h$ :

$$PB_1 = PB_0 \times e^{-2\alpha_{B1}h} \quad (1)$$

$$PY_1 = \frac{1}{2} \frac{\beta_1 \times PB_0}{\alpha_{B1} - \alpha_{Y1}} (e^{-2\alpha_{Y1}h} - e^{-2\alpha_{B1}h}) \quad (2)$$

While, these lights in dual-layer structure having  $h$  phosphor layer thickness are calculated with:

$$PB_2 = PB_0 \times e^{-2\alpha_{B2}h} \quad (3)$$

$$PY_2 = \frac{1}{2} \frac{\beta_2 \times PB_0}{\alpha_{B2} - \alpha_{Y2}} (e^{-2\alpha_{Y2}h} - e^{-2\alpha_{B2}h}) \quad (4)$$

In these expressions,  $h$  indicates the thickness of a phosphor film in the structure. By applying the subscripts "1" and "2", the single-layer and dual-layer remote configuration are described, respectively.  $\beta$  shows the conversion coefficient for the blue lights that convert to the yellow lights, while  $\gamma$  presents the yellow

lights' reflection coefficient.  $PB_0$  indicates the light intensity from blue LED formed by the intensities of blue light ( $PB$ ) and yellow light ( $PY$ ).  $\alpha_B$ ;  $\alpha_Y$  are parameters describing the energy loss fractions for blue and yellow lights throughout their propagation in the phosphor films, in turn. The optical performances of WLEDs utilizing the dual-layer phosphor geometry shows a considerable improvement compared to the single-layer structure:

$$\frac{(PB_2+PY_2)-(PB_1+PY_1)}{PB_1+PY_1} > 0 \quad (5)$$

Mie-scattering theory is used for the study of  $\text{LaAsO}_4:\text{Eu}^{3+}$  phosphor scattering effects and the computation of the scattering cross section  $C_{sca}$  for spherical particles as expressed in the following expression [22, 23]. Meanwhile, the Lambert-Beer law is used to compute the transmitted light power [24, 25]:

$$I = I_0 \exp(-\mu_{ext}L) \quad (6)$$

In which,  $I_0$  and  $L$  symbolize the incident light power and the thickness of each phosphor layer (mm), respectively. Meanwhile,  $\mu_{ext}$  indicates the extinction coefficient that can be reckoned following the expression of  $\mu_{ext} = N_r \cdot C_{ext}$ , where  $N_r$  ( $\text{mm}^{-3}$ ) means the number density distribution of particles, and  $C_{ext}$  ( $\text{mm}^2$ ) presents the extinction cross-section of phosphor particles.

From (5) we can see that with dual-layer remote phosphor structure WLEDs can yield much better luminous efficiency, compared to the single-layer one. Thus, the paper has demonstrated the efficiency of emitting luminous fluxes of this two-layered phosphor configuration. In fact, the double-layer remote structure gets their optical pathway significantly influenced by  $\text{LaAsO}_4:\text{Eu}^{3+}$  concentration values. Clearly, by applying the Beer's law, the reduction factor  $\mu_{ext}$  is in direct proportion to the concentration of  $\text{LaAsO}_4:\text{Eu}^{3+}$  but is in inverse ratio to the light transmission energy. Hence, as the thicknesses of two phosphor layers in WLEDs are fixed, the lumen output tends to decline when  $\text{LaAsO}_4:\text{Eu}^{3+}$  concentration goes up. As a result, Figure 6 shows a decrease in luminous flux in all 5 CCTs. When concentration of  $\text{LaAsO}_4:\text{Eu}^{3+}$  is at 26% wt. the lumen output significantly reduced. However, considering the advantages of the red phosphor class  $\text{LaAsO}_4:\text{Eu}^{3+}$  which are better CRI and CQS, and the better luminous output of this dual-layer remote phosphor geometry, compared to the results of the single-layer structure without the red phosphorus layer, the drawback in luminescence is perfectly acceptable. Finally, the decision is dependent on the goals of manufacturers, which gives the choice of suitable concentrations  $\text{LaAsO}_4:\text{Eu}^{3+}$  when producing these WLEDs in bulk.

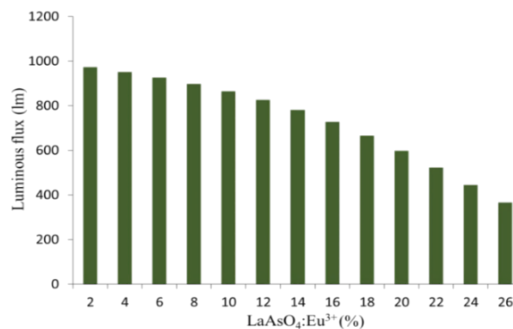


Figure 6. Luminous fluxes of WLEDs in accordance with  $\text{LaAsO}_4:\text{Eu}^{3+}$  concentrations

#### 4. CONCLUSION

The paper presents the effect of red phosphor  $\text{LaAsO}_4:\text{Eu}^{3+}$  on CRI and CQS of dual-layer phosphor structure. With the Mie-scattering theory and the Lambert-Beer rule, this article has confirmed the benefits in choosing  $\text{LaAsO}_4:\text{Eu}^{3+}$  for enhancing the color quality of WLEDs, which makes this red phosphor become one of the most appropriate solution to better LEDs' optical performance. The attained result works not only for WLEDs with a low color temperature but also for the ones with a high color temperature. Therefore, this research has fulfilled the given purposes, increasing the color quality of white light LEDs, which is very difficult to achieve with remote-phosphor structure. However, the luminous flux still has a significant degradation when concentration of  $\text{LaAsO}_4:\text{Eu}^{3+}$  increases excessively. Hence, the choice of an appropriate concentration becomes important, after carefully considering the goals of manufacturer. The study has provided much important information for reference in producing WLEDs for better color quality.

## REFERENCES

- [1] C. Tian, *et al.*, “Mn<sup>4+</sup>activated Al<sub>2</sub>O<sub>3</sub> red-emitting ceramic phosphor with excellent thermal conductivity,” *Opt. Express*, vol. 27, no.22, pp. 32666-32678, 2019.
- [2] X. D. Leng, *et al.*, “Feasibility of co-registered ultrasound and acoustic-resolution photoacoustic imaging of human colorectal cancer,” *Biomed. Opt. Express*, vol. 9, no. 11, pp. 5159-5172, November 2018.
- [3] H. S. E. Ghoroury, *et al.*, “Color temperature tunable white light based on monolithic color-tunable light emitting diodes,” *Opt. Express*, vol. 28, no. 2, pp. 1206-1215, 2020.
- [4] J. Cheng, *et al.*, “Photoluminescence properties of Ca<sub>4</sub>La<sub>6</sub>, SiO<sub>4.4</sub>, PO<sub>4.2</sub>O<sub>2</sub>-based phosphors for wLEDs,” *Chin. Opt. Lett.*, vol. 17, no. 5, pp. 051602, 2019.
- [5] Y. Yang, *et al.*, “Low complexity OFDM VLC system enabled by spatial summing modulation,” *Opt. Express*, vol. 27, no. 21, pp. 30788-30795, 2019.
- [6] L. He, *et al.*, “Performance enhancement of AlGaIn-based 365 nm ultraviolet light-emitting diodes with a band-engineering last quantum barrier,” *Opt. Lett.*, vol. 43, no. 3, pp. 515-518, February 2018.
- [7] Y. Wang, *et al.*, “Controlling optical temperature behaviors of Er<sup>3+</sup>doped Sr<sub>2</sub>CaWO<sub>6</sub> through doping and changing excitation powers,” *Opt. Mater. Express*, vol. 8, no. 7, pp. 1926-1939, July 2018.
- [8] J. Ji, *et al.*, “Theoretical analysis of a white-light LED array based on a GaN nanorod structure,” *Appl. Opt.*, vol. 59, no.8, pp. 2345-2351, 2020.
- [9] W. Wang, *et al.*, “On the development of an effective image acquisition system for diamond quality grading,” *Appl. Opt.*, vol. 57, no. 33, pp. 9887-9897, November 2018.
- [10] Y. F. Huang, *et al.*, “Red/green/blue LD mixed white-light communication at 6500K with divergent diffuser optimization,” *Opt. Express*, vol. 26, no. 18, pp. 23397-23410, 2018.
- [11] O. Kunieda, *et al.*, “High-quality full-parallax full-color three-dimensional image reconstructed by stacking large-scale computer-generated volume holograms,” *Appl. Opt.*, vol. 58, no. 34, pp. G104-G111, 2019.
- [12] A. Krohn, *et al.*, “LCD-Based optical filtering suitable for non-imaging channel decorrelation in VLC applications,” *Journal of Lightwave Technology*, vol. 37, no. 23, pp. 5892-5898, December 2019.
- [13] B. Qiu, *et al.*, “Synthesis and enhanced luminescent properties of SiO<sub>2</sub>@LaPO<sub>4</sub>:Ce<sup>3+</sup>/Tb<sup>3+</sup>microspheres,” *Optical Materials Express*, vol. 8, no. 1, pp. 59-65, 2018.
- [14] Y. Zhang, *et al.*, “Modeling and optimizing the chromatic holographic waveguide display system,” *Applied Optical*, vol. 58, no. 34, pp. G84-G90, 2019.
- [15] Q. T. Vinh, *et al.*, “Preliminary measure for the characterization of the usefulness of light sources,” *Optical Express*, vol. 26, no. 11, pp. 14538-14551, 2018.
- [16] H. P. Huang, *et al.*, “White appearance of a tablet display under different ambient lighting conditions,” *Opt. Express*, vol. 26, no. 4, pp. 5018-5030, 2018.
- [17] J. Chen, *et al.*, “Microlens arrays with adjustable aspect ratio fabricated by electrowetting and their application to correlated color temperature tunable light-emitting diodes,” *Opt. Express*, vol. 27, no. 4, pp. A25-A38, 2019.
- [18] C. McDonnell, *et al.*, “Grey-scale silicon diffractive optics for selective laser ablation of thin conductive films,” *Applied Optics*, vol. 57, no. 24, pp. 6966-6970, 2018.
- [19] A. D. Corbett, *et al.*, “Microscope calibration using laser written fluorescence,” *Optics Express*, vol. 26, pp. 21887-21899, 2018.
- [20] K. Orzechowski, *et al.*, “Optical properties of cubic blue phase liquid crystal in photonic microstructures,” *Optics Express*, vol. 27, no. 10, pp. 14270-14282, 2019.
- [21] S. J. Dain, *et al.*, “Lighting for color vision examination in the era of LEDs: the FM100Hue test,” *Journal of the Optical Society of America A*, vol. 37, no. 4, pp. A122-A132, 2020.
- [22] T. Hu, *et al.*, “Demonstration of color display metasurfaces via immersion lithography on a 12-inch silicon wafer,” *Opt. Express*, vol. 26, no.15, pp. 19548-19554, July 2018.
- [23] J. Ruschel, *et al.*, “Current-induced degradation and lifetime prediction of 310 nm ultraviolet light-emitting diodes,” *Photon. Res.*, vol. 7, no.7, pp. B36-B40, 2019.
- [24] A. A. Kaminari, *et al.*, “Linking infrared spectra of laboratory iron gall inks based on traditional recipes with their material components,” *Appl. Spectros.*, vol. 72, no. 10, pp. 1511-1527, May 2018.
- [25] M. E. Kandel, *et al.*, “Cell-to-cell influence on growth in large populations,” *Biomed. Opt. Express*, vol. 10, no.9, pp. 4664-4675, 2019.